Inorganic Chemistry

Communication

pubs.acs.org/IC

Single-Molecule Magnetism in a Pentacoordinate Cobalt(II) Complex Supported by an Antenna Ligand

Cyril Rajnák,[†] Ján Titiš,[†] Olaf Fuhr,[‡] Mario Ruben,[‡] and Roman Boča*[,†]

[†]Department of Chemistry, FPV, University of SS Cyril and Methodius, 917 01 Trnava, Slovakia

[‡]Institute of Nanotechnology, Karlsruhe Institute of Technology, 76344 Eggenstein-Leopoldshafen, Germany

Supporting Information

ABSTRACT: Pentacoordinate complex $[CoL^3Cl_2]$ with a tridentate antenna-like ligand L^3 forms a dimer held by short $\pi-\pi$ stacking with head-to-head contacts at 3.4 Å. The direct-current (dc) magnetic susceptibility and magnetization data confirm weak ferromagnetic interaction and a large-magnetic anisotropy, D/hc = 150 cm^{-1} and E/hc = 11.6 cm^{-1}. The system shows superparamagnetic behavior at low temperature that depends upon the applied magnetic field. At B_{dc} = 0.2 T, a low-frequency peak at the out-of-phase susceptibility is seen ($\nu \sim 0.3$ Hz), whereas the onset of the second peak appears at $\nu > 1500$ Hz, indicating the existence of two slow relaxation processes.

The family of known single-molecule magnets (SMMs) based on mononuclear 3d complexes is recently growing rapidly. These systems involve high-spin manganese(III), iron(III), iron(II), iron(I), and cobalt(II) complexes.[1−5] Just the last class attracts much attention for its versatility of coordination polyhedra and large magnetic anisotropy measured mainly by the axial zero-field-splitting parameter. Recently, a breakthrough has been achieved in the field of SMMs by using lanthanide centers such as terbium(III) and dysprosium(III), whose anisotropy can lead to extremely high relaxation barriers and which were even used as pivotal bricks in spintronic devices.[6] Several followup publications evoked the possibility that similar effects should be achievable with transition metals by controlling the magnitude of the d-orbital ligand-field-splitting energy.

The cobalt(II) SMM systems involve tri-,[5a] tetra-,[5b−e] penta-,[5f,g] and hexacoordinate[5h−l] complexes. The SMM behavior is usually visible under a small applied external field that suppresses the fast magnetic tunneling. The barrier to spin reversal is typically up to U/k_B = 40 K, and the extrapolated relaxation time is $\tau_0 = 10^{-10}-10^{-2}$ s [these two parameters enter the Arrhenius-like equation for the relaxation time $\tau = \tau_0 \exp(U/k_BT)$].

Herein we report about the single-molecule magnetism in new pentacoordinate complex $[CoL^3Cl_2]$, hereafter **1**, with a tridentate antenna-like ligand L^3. The ligand L^3 (4-hept-1-ynyl-2,6-dipyrazol-1-ylpyridine) has been prepared from 4-iodo-2,6-dipyrazol-1-ylpyridine and 1-heptyne by the procedure described in the Supporting Information (SI; Scheme 1). It was complexed with $CoCl_2 \cdot 6H_2O$ in CH_3CN, resulting in **1** (yield 74%).

The X-ray structure of **1** has been solved by standard procedures and refined to R_1 = 0.025 (see the SI). The SHAPE analysis shows a small deviation from the geometry of a tetragonal pyramid with one chloride ligand in the apical position. There are no hydrogen bonds, but two units are held together in a head-to-head fashion via short $\pi-\pi$ stacking at 3.37 Å; the Co···Co contacts are 5.66 Å (Figure 1).

Scheme 1. Preparation of the Ligand

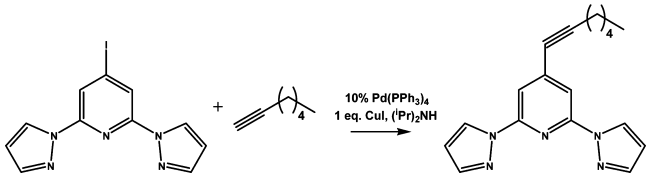

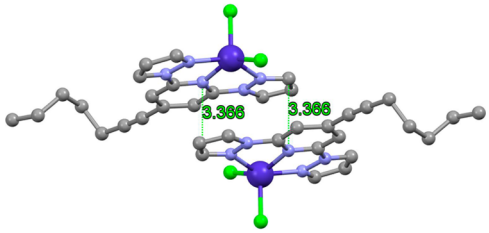

Figure 1. Two molecules of **1** showing short head-to-head contacts at 3.37 Å. Hydrogen atoms and the crystal solvent are hidden.

The direct-current (dc) magnetic data of **1** are displayed in Figure 2.[7] The room-temperature value of the effective magnetic

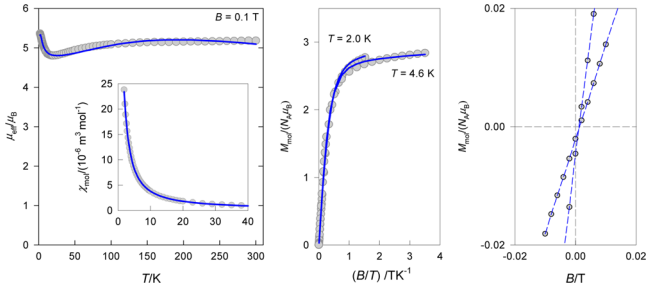

Figure 2. dc magnetic data for **1**: (left) temperature dependence of the effective magnetic moment (inset: temperature dependence of the molar magnetic susceptibility); (center and right) field dependence of the magnetization per mononuclear unit. Solid lines: fitted.

Received: June 27, 2014
Published: August 1, 2014

dx.doi.org/10.1021/ic501524a | Inorg. Chem. 2014, 53, 8200−8202

moment amounts to μ_{eff} = 5.18 μ_B; this high-temperature limit $\mu_{eff}(HT)/\mu_B = g_{iso}[S(S+1)]^{1/2}$ is recovered by a rather high value of g_{iso} = 2.67. On cooling, the effective magnetic moment decreases gradually, but below 30 K, it starts to increase. The magnetization per mononuclear formula unit $M_1 = M_{mol}/N_A\mu_B$ rises gradually with the applied field, and at T = 2.0 K and B = 7 T, it is M_1 = 2.8. There is no remnant magnetization in **1** in the time scale of the dc measurements: the magnetization curves taken at T = 4.6 and 2.0 K intercept near the zero field (a small shift of 0.17 mT is caused by the residual magnetic field of the setup that includes also the Earth magnetic field).

All attempts to fit the susceptibility and magnetization data to a conventional spin Hamiltonian for an $S = {}^3/_2$ system failed. The only successful fit was based upon an isotropic exchange in the dinuclear unit combined with large single-ion anisotropy (for details, see the SI). The correct powder average in the Zeeman term was secured by considering 120 orientations of the magnetic-field vector distributed uniformly over one hemisphere.

It was found that complex **1** possesses a small exchange coupling of the ferromagnetic nature (J/hc = +1.4 cm^{-1}) and very high single-ion magnetic anisotropy expressed by the axial zero-field-splitting parameter D/hc = 151 cm^{-1} and its rhombic counterpart E/hc = 11.6 cm^{-1} (g_z = 2.00; $g_{x,y}$ = 3.28). High-positive values of the D parameters are typical for hexa- and pentacoordinate cobalt(II) complexes.[8] A small positive exchange coupling constant has been confirmed also by density functional theory (DFT) calculations.[9]

It is generally accepted that a negative value of the D parameter is a prerequisite of SMM behavior. However, SMM behavior has also been reported for mononuclear tetra- and hexacoordinate cobalt(II) complexes with positive D.[5c,h,j] For such a reason, we probed the SMM behavior of our pentacoordinate complex **1** with positive finding.

The alternating-current (ac) susceptibility measurements for complex **1** are displayed in Figure 3; at T = 2.0 K, the out-of-

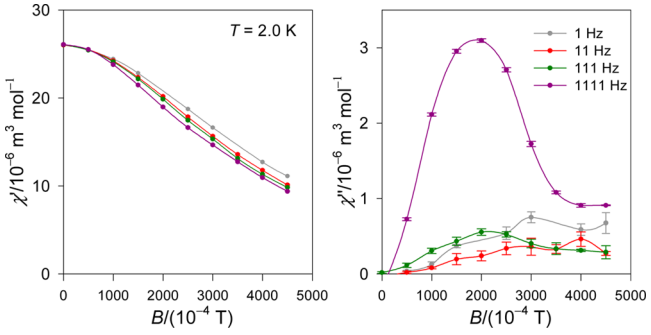

Figure 3. ac susceptibility data for **1** at T = 2.0 K as a function of the applied dc magnetic field for four frequencies.

phase susceptibility when plotted versus the magnetic induction displays a maximum that is frequency-dependent. Because the maximum was localized around B_{dc} = 0.2 T, subsequent measurements have been done at this field.

Figure 4 shows a frequency dependence of the in-phase and out-of-phase components of the ac magnetic susceptibility for 22 frequencies ranging between 0.04 and 1512 Hz for a number of temperatures. At low frequencies ($\nu \sim$ 3 Hz), a well-developed maximum is seen, whereas the second maximum will lie above 1500 Hz. A generalized Debye model was used in fitting the ac susceptibility data. The fitting procedure was based on

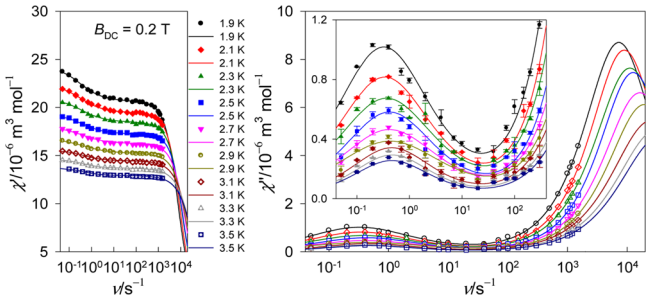

Figure 4. Frequency dependence of the ac susceptibility for **1** at B_{dc} = 0.2 T: (left) in-phase component; (right) out-of-phase component. Solid lines: fitted with the model of two relaxation processes.

minimization of a functional $F = w_1R(\chi') + w_2R(\chi'')$, which accounts for relative errors of both data sets ($R < 0.05$).

The actual model contains relaxation times (τ_i), distribution parameters (α_i), and isothermal susceptibilities (χ_{Ti}) along with the adiabatic susceptibility (χ_S) for individual relaxation processes. The model with two relaxation processes has been applied, and the data in the numerical form are deposited in the SI; they yield the convolution lines depicted in Figure 5.

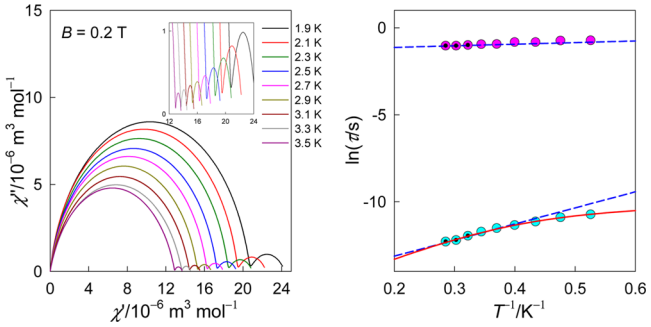

Figure 5. Fitted ac susceptibility data for **1** at B_{dc} = 0.2 T: (left) Argand diagram (fixed temperature; lines: calculated upon fitted parameters); (right) Arrhenius-like plot. Coefficients of the linear regression (blue, dashed) ln $\tau = a + b/T$: a = ln τ_0 and $b = U/k_B$.

The plot of χ'' versus χ' (the Argand diagram) is shown in Figure 5. This, in fact, is represented by two arcs of different height and compression (α_i). The positions of the maxima of the deconvolution (primitive) curves at ν''_{max} enter the Arrhenius-like equation of the thermal activation process, i.e., ln τ = ln(1/$2\pi\nu''_{max}$) versus $1/T$. Then the linear fit for three higher-temperature points yields the parameters of the SMM at B_{dc} = 0.2 T. The faster relaxation process at the higher temperature is characterized by the extrapolated relaxation time $\tau_0^{(2)} = 3.12 \times 10^{-7}$ s and barrier to spin reversal $U^{(2)}/k_B$ = 9.2 K. The lower-temperature process is much slower with $\tau_0^{(1)}$ = 0.27 s and $U^{(1)} \sim$ 0.9 K.

The fitting procedure was done also by using an extended model that involves the direct (D), Raman (R), and the Orbach (O) processes according to eq 1.

$$\tau^{-1} = AB^2T + CT^n + \tau_0^{-1}\exp(-\Delta E/T) \quad (1)$$

The resulting parameters $A = 5.2 \times 10^6$ T^{-2} K^{-1} s^{-1}, $C = 1.0 \times 10^{-3}$ K^{-4} s^{-1} for n = 4, ΔE = 13.54 K, and $\tau_0^{-1} = 7.4 \times 10^6$ s recover the experimental data almost perfectly (red, solid line in Figure 5, right). To this end, $\tau_0^{(2)} = 1.35 \times 10^{-7}$ and $U^{(2)}/k_B$ = 13.5 K were obtained.

dx.doi.org/10.1021/ic501524a | Inorg. Chem. 2014, 53, 8200−8202

The application of a small field (B_{dc} = 0.2 T) is essential in suppressing the magnetic tunneling mechanism, which gives a much faster relaxation process. The existence of two slow relaxation processes can be attributed to the relaxation of the dimeric units $[CoL^3Cl_2]_2$ that are weakly exchange-coupled (the slower process, $\tau_0 \sim 10^{-2}$ s) proceeding at low temperature; the faster process, $\tau_0 \sim 10^{-7}$ s, is attributed to the relaxation of uncoupled monomers $[CoL^3Cl_2]$.

The fitting procedure applied to the ac susceptibility data (both χ'' and χ') is essential in a proper characterization of the relaxation processes. The barrier to spin reversal for the case of $D > 0$ is governed by the rhombic anisotropy parameter E that is essential in modifying the easy plane of magnetization and the presence of an orientational axis (see Figure S8 in the SI).[5h]

In conclusion, the pentacoordinate cobalt(II) complex **1**, forming a dimer through $\pi-\pi$ stacking, belongs to the family of 3d complexes showing single-molecule magnetism. It exhibits two slow relaxation processes of which the faster one possesses characteristics typical for this class of complexes.

■ ASSOCIATED CONTENT

Supporting Information

Experimental details and figures/tables referring to the synthesis and analytical, structural (CCDC 953194), and magnetic data. This material is available free of charge via the Internet at http://pubs.acs.org.

■ AUTHOR INFORMATION

Corresponding Author

*E-mail: roman.boca@stuba.sk.

Notes

The authors declare no competing financial interest.

■ ACKNOWLEDGMENTS

Grant agencies (Slovakia: VEGA 1/0233/12, VEGA 1/0522/14, and APVV-0014-11) are acknowledged for financial support. C.R. acknowledges the Institute de Physique et Chimie des Matériaux (Strasbourg) and facilities at Karlsruhe Institute of Technology (Germany).

■ REFERENCES

(1) (a) Ishikawa, R.; Miyamoto, R.; Nojiri, H.; Breedlove, B. K.; Yamashita, M. *Inorg. Chem.* **2013**, *52*, 8300. (b) Grigoropoulous, A.; Pissas, M.; Rapatolis, P.; Psycharis, V.; Kyritsis, P.; Sanakis, Y. *Inorg. Chem.* **2013**, *52*, 12869. (c) Vallejo, J.; Pascual-Alvarez, A.; Cano, J.; Castro, I.; Julve, M.; Lloret, F.; Krzystek, J.; De Munno, G.; Armentano, D.; Wernsdorfer, W.; Ruiz-Garcia, R.; Pardo, E. *Angew. Chem., Int. Ed.* **2013**, *52*, 14075.

(2) Mossin, S.; Tran, B. L.; Adhikari, D.; Pink, M.; Heinemann, F. W.; Sutter, J.; Szilagyi, R. K.; Meyer, K.; Mindiola, D. J. *J. Am. Chem. Soc.* **2012**, *134*, 13651.

(3) (a) Harman, W. H.; Harris, T. D.; Freedman, D. E.; Fong, H.; Chang, A.; Rinehart, J. D.; Ozarowski, A.; Sougrati, M. T.; Grandjean, F.; Long, G. J.; Long, J. R. *J. Am. Chem. Soc.* **2010**, *132*, 18115. (b) Freedman, D. E.; Harman, W. H.; Harris, T. D.; Long, G. J.; Chang, C. J.; Long, J. R. *J. Am. Chem. Soc.* **2010**, *132*, 1224. (c) Weismann, D.; Sun, Y.; Lan, Y.; Wolmershauser, G.; Powell, A. K.; Sitzmann, H. *Chem.—Eur. J.* **2011**, *17*, 4700. (d) Lin, P.-H.; Smythe, N. C.; Gorelsky, S. J.; Maguire, S.; Henson, N. J.; Korobkov, I.; Scott, B. L.; Gordon, J. C.; Baker, R. T.; Murugesu, M. *J. Am. Chem. Soc.* **2011**, *133*, 15806.

(4) Zadrozny, J. M.; Xiao, D. J.; Atanasov, M.; Long, G. J.; Grandjean, F.; Neese, F.; Long, J. R. *Nat. Chem.* **2013**, *5*, 577.

(5) (a) Eichhofer, A.; Lan, Y.; Mereacre, V.; Bodenstein, T.; Weigend, F. *Inorg. Chem.* **2014**, *53*, 1962. (b) Zadrozny, J. M.; Long, J. R. *J. Am. Chem. Soc.* **2011**, *133*, 20732. (c) Zadrozny, J. M.; Liu, J.; Piro, N. A.; Chang, C. J.; Hill, S.; Long, J. R. *Chem. Commun.* **2012**, *48*, 3927. (d) Yang, F.; Zhou, Q.; Zhang, Y.; Zeng, G.; Li, G.; Shi, Z.; Wang, B.; Feng, S. *Chem. Commun.* **2013**, *49*, 5289. (e) Boča, R.; Miklovič, J.; Titiš, J. *Inorg. Chem.* **2014**, *53*, 2367. (f) Jurca, T.; Farghal, A.; Lin, P.-H.; Korobkov, I.; Murugesu, M.; Richeson, D. S. *J. Am. Chem. Soc.* **2011**, *133*, 15814. (g) Habib, F.; Luca, O. R.; Vieru, V.; Shiddiq, M.; Korobkov, I.; Gorelsky, S. I.; Takase, M. K.; Chibotaru, L. F.; Hill, S.; Crabtree, R. H.; Murugesu, M. *Angew. Chem., Int. Ed.* **2013**, *52*, 11290. (h) Vallejo, J.; Castro, I.; Ruiz-Garcia, J.; Cano, J.; Julve, M.; Lloret, F.; De Munno, G.; Wernsdorfer, W.; Pardo, E. *J. Am. Chem. Soc.* **2012**, *134*, 15704. (i) Colacio, E.; Ruiz, K.; Ruiz, E.; Cremades, E.; Krzystek, J.; Carretta, S.; Cano, J.; Guidi, T.; Wernsdorfer, W.; Brechin, E. K. *Angew. Chem., Int. Ed.* **2013**, *52*, 9130. (j) Zhu, Y.-Y.; Cui, C.; Zhang, Y.-Q.; Jia, J.-H.; Guo, X.; Gao, C.; Qian, K.; Jiang, S.-D.; Wang, B.-W.; Wang, Z.-M.; Gao, S. *Chem. Sci.* **2013**, *4*, 1802. (k) Gass, I. A.; Tewary, S.; Nafady, A.; Chilton, N. F.; Gartshore, C. J.; Asadi, M.; Lupton, D. W.; Moubaraki, B.; Bond, A. M.; Boas, J. F.; Guo, S.-X.; Rajaraman, G.; Murray, K. S. *Inorg. Chem.* **2013**, *52*, 7557. (l) Herchel, R.; Váhovská, L.; Potočňák, I.; Trávníček, Z. *Inorg. Chem.* **2014**, *53*, 5896.

(6) (a) Ishikawa, N.; Sugita, M.; Okubo, T.; Tanaka, N.; Iino, T.; Kaizu, Y. *Inorg. Chem.* **2003**, *42*, 2440. (b) Branzoli, F.; Carretta, P.; Filibian, M.; Zoppellaro, G.; Graf, M. J.; Galan-Mascaros, J. R.; Fuhr, O.; Brink, S.; Ruben, M. *J. Am. Chem. Soc.* **2009**, *131*, 4387. (c) Urdampilleta, M.; Cleuziou, J.-P.; Klyatskaya, S.; Ruben, M.; Wernsdorfer, W. *Nat. Mater.* **2011**, *10*, 502. (d) Vincent, R.; Klyatskaya, S.; Ruben, M.; Wernsdorfer, W.; Balestro, F. *Nature* **2012**, *488*, 357. (e) Ganzhorn, M.; Klyatskaya, S.; Ruben, M.; Wernsdorfer, W. *Nat. Nanotechnol.* **2013**, *8*, 165.

(7) The magnetic data were measured with a SQUID apparatus (MPMS-XL7, Quantum Design) using the detection in the reciprocating sample option; ca. 22 mg of the sample was encapsulated in a gelatin sample holder. The molar susceptibility taken at B = 0.1 T was corrected for the underlying diamagnetism. The dc magnetization has been measured in the field-decreasing mode in order to detect an eventual remnant magnetization. The ac susceptibility measurements were done with an oscillating field B_{AC} = 0.38 mT for 22 frequencies; 10 scans were averaged for each temperature-frequency point.

(8) (a) Titiš, J.; Boča, R. *Inorg. Chem.* **2011**, *50*, 11838. (b) Idešicová, M.; Boča, R. *Inorg. Chim. Acta* **2013**, *408*, 162. (c) Rajnák, C.; Titiš, J.; Šalitroš, I.; Boča, R.; Fuhr, O.; Ruben, M. *Polyhedron* **2013**, *65*, 122. (d) Hudák, J.; Boča, R.; Moncol, J.; Titiš, J. *Inorg. Chim. Acta* **2013**, *394*, 401.

(9) The dimeric unit consisting of 62 atoms in its experimental geometry has been calculated by the *ORCA* program[10] using the TZV basis set (17s11p6d1f) → [6s4p3d1f] for cobalt, (14s9p1d) → [5s5p1d] for chlorine, (11s6p1d) → [5s3p1d] for nitrogen and carbon, and (5s) → [3s] for hydrogen and the appropriate set of auxiliary functions. DFT calculations (B88 and P86) with the broken-symmetry approach gave J/hc = 0.36 cm^{-1}.

(10) Neese, F. *ORCA 2.8*; University Bonn: Bonn, Germany, 2008.